Ab initio pseudopotential calculation of the photo-response of metal clusters

J. M. Pacheco[a)]
Departamento de Fisica da Universidade, 3000 Coimbra, Portugal

José Luís Martins[b)]
Departamento de Física, Instituto Superior Técnico, Avenida Rovisco Pais 1, 1096 Lisboa, Portugal and INESC, Rua Alves Redol, 9, 1000 Lisboa Codex, Portugal

(Received 14 August 1996; accepted 31 December 1996)

The photoabsorption cross section of small sodium and lithium clusters is computed in the time-dependent local density approximation to density functional theory, making use of two different types of *ab initio* nonlocal pseudopotentials. The equilibrium geometries of the clusters have been obtained via Langevin quantum molecular dynamics. It is found that the average bond length of the clusters and their static polarizabilities depend on the input pseudopotential. Nonetheless, it is found that the different pseudopotentials lead to the *same* equilibrium shape for the clusters, and to multipeaked line shapes for the photoabsorption cross sections which are nearly identical, apart from small overall energy shifts. For sodium, it is found that the local reduction of the pseudopotential obtained by keeping only its s-part provides, in all cases, an excellent approximation to the full pseudopotential, whereas for lithium the same procedure proves inaccurate. © *1997 American Institute of Physics.* [S0021-9606(97)01913-2]

I. INTRODUCTION

The last decade has witnessed a great improvement on the experimental methods and techniques for studying free alkali metal clusters, providing theorists with a wealth of new experimental data on which to test well established methods and approximations (for a review, see Ref. 1). In this respect, *ab initio* density functional theory (DFT) calculations, making use of norm-conserving, nonlocal pseudopotentials, constitute a state-of-the-art technique which allows an unbiased search for global and local minima in the potential energy hypersurface of clusters. Indeed, DFT, in the local spin density approximation (LSDA), has been recently employed[2] in the study of size-dependent structural and electronic properties of lithium clusters over a range which grows from the dimer to clusters with up to 150 atoms. These calculations come in line with previous but more limited studies carried out for sodium clusters by other authors,[3,4] and reflect the increase of usage, as well as the development of such methods in the study of structural and electronic properties of clusters.

The theoretical study of optical properties of clusters, making use of *ab initio* pseudopotentials and including explicitly the discrete ionic skeleton, has not paralleled the status reached in structural minimization, and has been applied only to few, specific clusters,[5–7] making use of a linear response theory in LDA-DFT, known as time-dependent LDA (TDLDA). Therefore, a good deal of our understanding of fine-structure features of the optical response of metal clusters, which display pronounced quantum size effects, relies on original theoretical predictions[8] making use of a structureless model—the spherical jellium model (SJM).

The static polarizability of a metal cluster (and, via the usual Kramers–Kronig relations, the centroid of the surface plasmon) is very sensitive to the cluster volume, scaling linearly with it. The effective volume of a cluster, in turn, is directly related to the issue of lattice contraction in finite metal particles, which is still a matter of debate.[9] In the SJM, the cluster volume is usually fixed from the outset (via the Wigner Seitz radius r_s). In an *ab initio* framework the size of the cluster should be determined from a minimization of the total energy of the system with respect to the coordinates of all the constituent atoms.

A qualitative measure of the cluster volume is provided, for a given geometry (and for the smaller clusters), by the value of the average nearest-neighbor bond length obtained as a result of the total-energy minimization.[4] In Fig. 1, inspired by Fig. 15 of Ref. 4, we compiled the average bond length of neutral sodium clusters, for selected sizes from Na_2 to Na_{20}, obtained via structural minimization within DFT and making use of different pseudopotentials. The experimental knowledge is restricted to the two limiting cluster sizes, the dimer[10] and the bulk,[11] which are also represented. From Fig. 1 it is clear that different pseudopotentials may lead to different average bond lengths, and thus different delocalization volumes for the valence electrons of clusters. *Ab initio* pseudopotentials are typically nonlocal. This nonlocality—which naturally arises when it is required that the pseudopotential correctly mimics the scattering properties of the all-electron atom—determines, among other effects, the nature of the chemical bonding between atoms in any many-atom system, being directly responsible for, e.g., the directional character of the bond in many semiconductor and insulating materials. Therefore, it is of interest to investigate the role played by *ab initio* nonlocal pseudopotentials in the prediction of the optical response of clusters. This is

a)Electronic address: pacheco@hydra.ci.uc.pt
b)Electronic address: jose.l.martins@inesc.pt

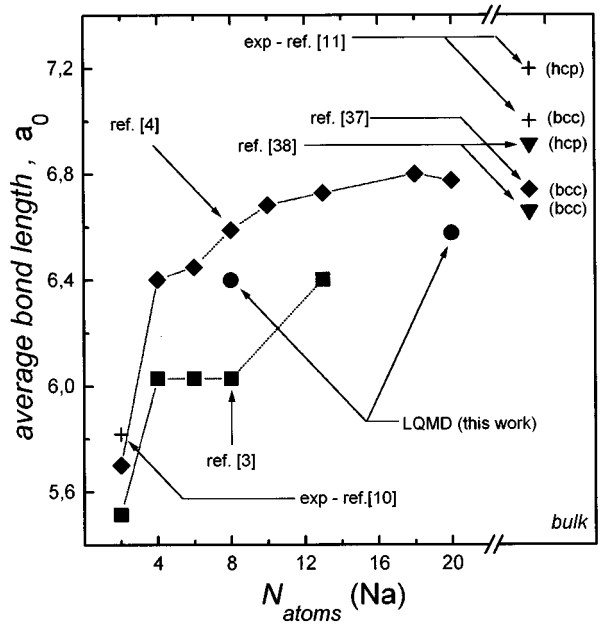

FIG. 1. The average nearest-neighbor bond length of neutral sodium clusters is shown as a function of the number of atoms. This value is calculated as in Ref. 4, namely, it corresponds to the arithmetic average of nearest-neighbor bondlengths, within cutoff distance of 7.7 a.u. The experimental values (known for the dimer and bulk) are represented by crosses. The diamonds correspond to the results obtained in Ref. 4 making use of the Car-Parrinello method, using a BHS-type pseudopotential (see main text for details and definitions). The bulk-bcc value (Ref. 37) has been obtained with the same pseudopotential. The squares correspond to the structural minimization carried out in Ref. 3, making use of the BHS pseudopotential also used in this work. The circles correspond to the results of the present work obtained via LQMD and using the TM pseudopotentials. Finally, the triangles correspond to the bulk calculation of Ref. 38.

the purpose of the present paper, in which we study the optical properties of alkali clusters and their relation to the choice of input pseudopotential. To this end, we selected four magic clusters—Na_8, Na_{20}, Li_8, and Li_{20}—and computed their photoabsorption cross section making use of two different *ab initio* pseudopotentials: The pseudopotentials tabulated by Bachelet, Hamman, and Schlüter[12] (BHS), and generated following the recipe of Troullier and Martins[13] (TM). The optimal geometries associated with each pseudopotential were determined within the LDA-DFT using a Langevin quantum molecular dynamics[14] (LQMD) simulated annealing. Since both pseudopotentials were constructed using the Perdew and Zunger parametrization[15] of the Ceperley–Alder results[16] for the exchange and correlation (XC), we adopted the same XC functional both for the structural minimization as well as for the computation of the TDLDA optical response.

The outline of this paper is the following: In Sec. II the theoretical framework and computational method are reviewed. Section III is devoted to the discussion of the results obtained and comparison with available experimental data, whereas in Sec. IV the main conclusions and future prospects are summarized.

II. THEORY

A. Structural minimization

In order to find the equilibrium positions $\{\mathbf{R}_i\}$ for the constituent atoms of the cluster, we use the Langevin quantum molecular dynamics (LQMD) method developed in Ref. 14, which allows the study of structural properties of complex systems. LQMD can be used to perform finite-temperature simulations and evaluate properties as a function of temperature. This constitutes a key ingredient in the study of metallic clusters (cf. e.g., Refs. 4, 17, and the recent experimental data in Ref. 18).

Starting from a set of positions specified by the N vectors $\{\mathbf{R}_i\}$, the ionic positions evolve in time according to the Langevin equation

$$M_i \frac{d^2\mathbf{R}_i}{dt^2} = -\nabla_{\mathbf{R}_i} E(\{\mathbf{R}_i\}) - \gamma M_i \frac{d\mathbf{R}_i}{dt} + \mathbf{G}_i , \tag{1}$$

where $E(\{\mathbf{R}_i\})$ is the total energy of the system calculated from LDA-DFT and M_i is the ionic mass. The last two terms on the right hand side are the Langevin dissipation and fluctuation forces defined, respectively, by the friction coefficient γ and the distribution of the random Gaussian variables $\{\mathbf{G}_i\}$, determined from the fluctuation-dissipation theorem. The total energy $E(\{\mathbf{R}_i\})$ and the forces $-\nabla_{\mathbf{R}_i} E(\{\mathbf{R}_i\})$ are determined via efficient self-consistent pseudopotential plane-wave calculations, in which the pseudopotentials are cast into the Kleinman–Bylander separable form,[19] so that a fast iterative diagonalization procedure can be used to find the LDA-DFT self-consistent solution at each time step.

B. Optical response

Once the set of equilibrium ionic positions $\{\mathbf{R}_i\}$ has been determined for each pseudopotential, we are now in a condition to compute the optical response of the metal clusters with the TDLDA. In general, the ionic field can be highly anisotropic, and the computation of the optical response in TDLDA is considerably more time consuming than the LDA-DFT computation of the ground-state solution. In this paper, we consider only ''magic'' metallic clusters, for which this anisotropy is minimal, and we make the approximation of rotationally averaging the ionic field, with great savings in computing time. For the purpose of the present study, it is not necessary to include in full detail the anisotropic terms, which can be reintroduced perturbatively.[20] Therefore, starting from the equilibrium positions $\{\mathbf{R}_i\}$, we solve the LDA Kohn–Sham equations, expanding the solutions in a spherical basis set, obtained by solving the corresponding SJM problem.[21] This technique has proved successful in the computation of the optical response of such diverse systems as jellium metal clusters,[22,23] fullerenes,[6] and metal-coated fullerenes.[7] Once the LDA one-electron energies and wave functions are obtained, we proceed to the computation of the optical response in TDLDA.

The central quantity to be computed in the TDLDA response to an external photon field is the (complex) polarizability

$$\alpha(E) = -\sum_n |\langle n|\hat{D}|0\rangle|^2 \left[\frac{1}{E-E_n+i\eta} - \frac{1}{E+E_n+i\eta}\right], \tag{2}$$

where η is a positive infinitesimal and $\hat{D}=e\hat{z}$ is the dipole photon field. $|n\rangle$ are the TDLDA excited states (with excitation energies E_n), solutions of the following eigenvalue problem (for details, see Ref. 22):

$$\begin{pmatrix} A & B \\ -B^* & -A^* \end{pmatrix} \begin{pmatrix} X_{ph}^{(n)} \\ Y_{ph}^{(n)} \end{pmatrix} = E^{(n)} \begin{pmatrix} X_{ph}^{(n)} \\ Y_{ph}^{(n)} \end{pmatrix}. \tag{3}$$

The matrices A and B are defined as

$$A_{ph,p'h'} = (e_p - e_h)\,\delta_{p,p'}\,\delta_{h,h'} + \langle ph'|V_{ph}|p'h\rangle, \tag{4}$$

$$B_{ph,p'h'} = \langle pp'|V_{ph}|h'h\rangle, \tag{5}$$

where $e_p(e_h)$ are LDA electron (hole) orbital energies, and V_{ph} is the residual electron-hole interaction, which is responsible for the screening of the photon field and is given by

$$V_{ph}(\mathbf{r},\mathbf{r}_1) = \frac{e^2}{|\mathbf{r}-\mathbf{r}_1|} + \frac{\delta V_{\rm xc}|n(\mathbf{r})|}{\delta n}\,\delta(\mathbf{r}-\mathbf{r}_1). \tag{6}$$

The transition matrix elements in Eq. (2) are then obtained from the unscreened electron-hole transitions by

$$\langle n|\hat{D}|0\rangle = \sum_{ph} (X_{ph}^{(n)} - Y_{ph}^{(n)})\langle p|\hat{D}|h\rangle. \tag{7}$$

Finally, the photoabsorption cross section can be straightforwardly obtained from the polarizability defined in Eq. 2 via the relation

$$\sigma(E) = \frac{4\pi E}{\hbar c}\,\mathrm{Im}[\alpha(E)]. \tag{8}$$

III. RESULTS AND DISCUSSION

A. Ground-state properties

We used LQMD in order to carry out the structural minimization of the four clusters, in LDA-DFT, using both the BHS and the TM pseudopotentials. We adopted the original parametrization of Ref. 12 for the BHS pseudopotentials. For the TM soft pseudopotential, the key ingredient is the cutoff radius r_c, which may be l dependent. Indeed, for lithium we used $r_c=1.9$ a.u. and $r_c=2.1$ a.u. for $l=0$ and $l=1$, respectively, whereas for sodium we use the same value, $r_c=2.6$ a.u., for both scattering channels.

In the LQMD simulations, we start with an initial thermal bath temperature of 400 K, the cluster being gradually cooled down to a final bath temperature of 10 K, in constant steps of 39 K. At each temperature stage we perform 40 molecular dynamics steps. The simulation conditions used were similar for all runs, namely, we used an fcc supercell with lattice constant of $a=40$ a.u., an energy cutoff of 9 Ry, a Langevin friction parameter $\gamma=5\times10^{-4}$ a.u., and a time step of 500 a.u. As appropriate for cluster simulations, only the Γ point has been considered in the sampling of reciprocal space of the supercell, and a Gaussian level broadening of 0.02 Ry has been used. In line with Ref. 14, at the end of the LQMD simulation, we finished the optimization of the geometry by a conjugate gradient method.

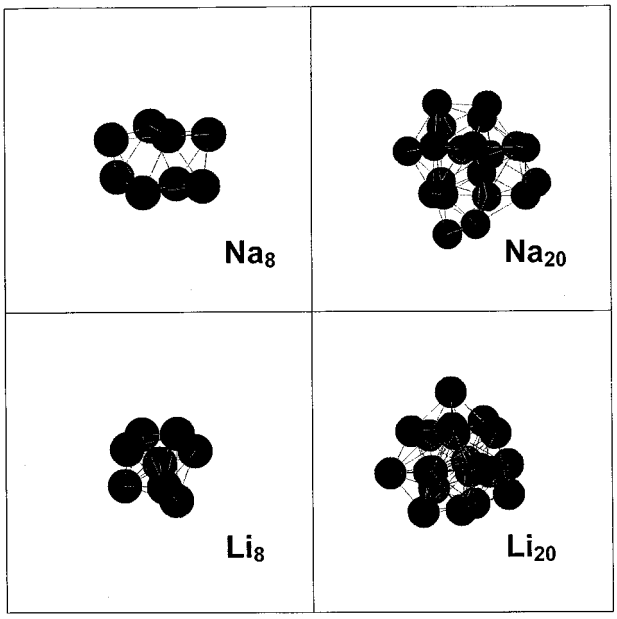

FIG. 2. Geometrical shapes of the calculated equilibrium configuration are shown for the four clusters considered in this work. The two pseudopotentials lead to the same geometrical shapes but somewhat different bond lengths.

Figure 2 shows the equilibrium structures calculated for the four clusters. Their shape is essentially independent of the choice of pseudopotential, but there is some dependence of the cluster size on the pseudopotential. The symmetries of the calculated equilibrium geometries are the same as those obtained previously for sodium[3] and lithium[2] within the LDA, namely, the bicapped octahedron for Na_8, the centered trigonal prism for Li_8; the two structures obtained for the 20-atom clusters are more difficult to classify. Even though the geometrical shape is the same, the bond lengths calculated using the BHS pseudopotential are smaller than the bond lengths calculated with the TM pseudopotential. Inspecting the calculated average bond length $d_{\rm av}$ shown in Table I, we can see that the difference is sizeable for the sodium clusters, but minor in the lithium case.

To investigate the dependence of cluster size on pseudopotential, we tested the sensitivity of the equilibrium shape of Na_8 on the parameters controlling the construction of the two pseudopotentials. For the TM pseudopotential we constructed a few pseudopotentials using different values of the input cutoff radius r_c and found that the results are quite insensitive to that parameter. For the case of the BHS pseudopotential we found that if we use in the generation of the pseudopotential the ground-state atomic configuration instead of the highly ionized p-orbital configuration used to generate the BHS tables, we get an average bond length of 6.39 for Na_8, in much better agreement with the value of 6.38 obtained with the TM pseudopotential. These results seem to indicate that the TM pseudopotentials are more suit-

TABLE I. The table shows the average nearest-neighbor bond length, d_{av} and the static polarizability $\overline{\alpha}/\alpha_{cl}$ of the magic clusters Li_8, Li_{20}, Na_8, and Na_{20} calculated for two different pseudopotentials. Two values are given for the static polarizability. The one obtained with the full nonlocal pseudopotential and, in parenthesis, the one obtained by the local reduction of the same pseudopotential. Whenever available, the experimental value for the rotationally averaged static polarizability is also given.

		Static properties		
Cluster	PSP	$d_{av}(a_0)$	$\overline{\alpha}/\alpha_{cl}$	$\overline{\alpha}_{exp}/\alpha_{cl}$
Na_8	BHS	6.04	1.44 (1.43)	1.72±0.03
Na_8	TM	6.38	1.55 (1.55)	1.72±0.03
Na_{20}	BHS	6.15	1.27 (1.27)	1.58±0.04
Na_{20}	TM	6.59	1.47 (1.46)	1.58±0.04
Li_8	BHS	5.00	1.93 (1.93)	
Li_8	TM	5.02	1.93 (1.93)	
Li_{20}	BHS	5.50	1.58 (1.57)	
Li_{20}	TM	5.52	1.58 (1.57)	

able to provide bias-free results in electronic structure calculations.

The difference in the average bond length implies that the effective volume of the BHS clusters is smaller than that of the TM clusters, leading to a corresponding difference in the static polarizability of those systems. We computed this quantity along the lines of Sec. II, taking into account that the static polarizability can be obtained immediately from Eq. (2) making $E=0$. In Table I we listed the calculated average polarizability divided by the polarizability of a classical spherical metal particle, $\alpha_{cl}=r_s^3N$, where r_s is the bulk Wigner–Seitz radius, and N is the number of atoms in the cluster,[24] for the four clusters being studied and for the two pseudopotentials.

Before comparing our results with experimental data for sodium,[25] we should discuss the three approximations used in this work that can affect the calculated average bond length and, correspondingly, the static polarizability. (i) Thermal effects: These have not been included in our theoretical treatment,[26] whereas the experimental data of Ref. 25 has been obtained in hot, liquidlike clusters, with a vibrational temperature of the order of 300 K.[17] At this temperature, the thermal expansion of clusters[27] provides a measurable contribution to the average polarizability of clusters. (ii) Linearization of the XC term: The XC term is a highly nonlinear function of the density, which is typically linearized in the unscreening of the pseudopotential.[13,28] This linearization has been shown to lead to a reduction of the average bond length of dimers of alkali clusters,[29] as well as for larger metal clusters.[4] (iii) Self-interaction errors; These errors, which are inherent in LDA, have been shown to affect both structural minimization of clusters[30] as well as the static and dynamical polarizability of clusters.[31] In particular, there is an increase of the static polarizability of metal clusters.

All effects described above will increase the average static polarizability of a metal cluster. Therefore, it is rewarding that the results obtained in this paper do underestimate the experimental values of the average static polarizabilities.

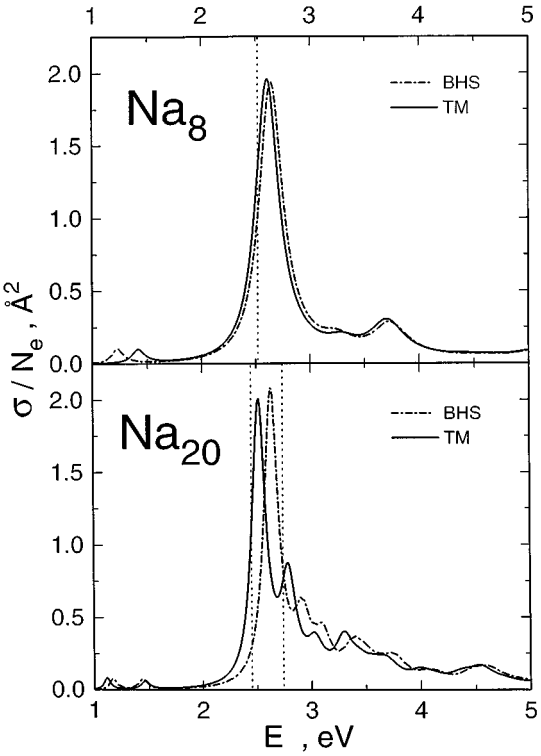

FIG. 3. The photoabsorption cross section per valence electron (in Å^2) for Na clusters computed with the BHS pseudopotential (dashed lines) and with the TM pseudopotential (full lines) are plotted as a function of photon energy (in eV). The calculations take into account the underlying ionic structure. The vertical lines indicate the energy position of the main peaks dominating the lineshape of the cross section measured experimentally (Ref. 39).

B. Optical response

Starting from the geometries obtained in the previous section, we computed the photoabsorption cross section for all clusters. The results are shown in Figs. 3 and 4 for sodium and lithium, respectively. With dashed lines, the line shape of the photoabsorption cross section per particle computed with the BHS pseudopotentials is drawn, whereas the corresponding quantity computed with the TM pseudopotential is drawn with full lines.[32] For the two sodium clusters, as well as for the lithium octamer, vertical dashed lines are placed at the energies corresponding to the most important peaks determined experimentally. For both lithium and sodium clusters, the line shapes obtained with the two pseudopotentials are remarkably similar, in spite of the rather different effective volumes which result from the geometry optimization. Indeed, in the plasmon pole approximation one would expect an energy shift of the absorption peak (the plasmon peak) toward the red as the volume of the cluster increases. In our calculation, these energy shifts are only reminiscent of the different effective volumes, being negligible in the case of Na_8, for which one might expect a plasmon-pole type of argument to be relevant. This feature is directly related to the nonlocal nature of the pseudopotentials, and not only reveals a nontrivial correspondence between the cluster effective volume and the photoabsorption

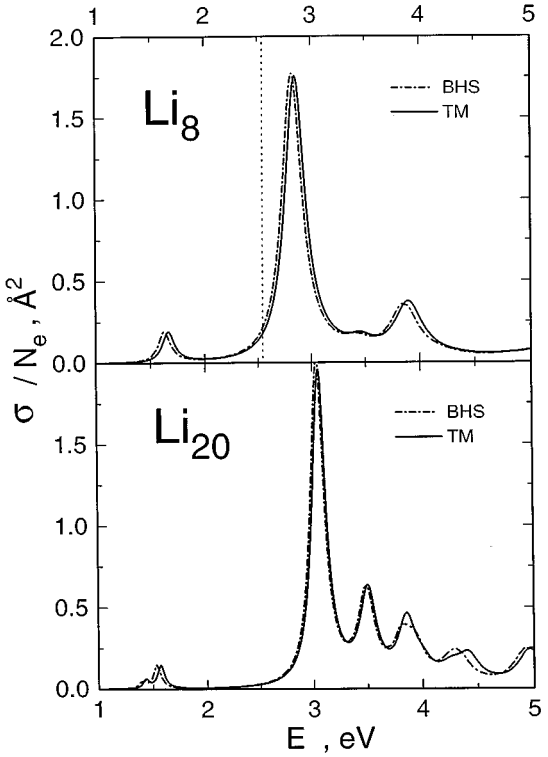

FIG. 4. The photoabsorption cross section per valence electron (in $Å^2$) for lithium clusters computed with the BHS pseudopotential (dashed lines) and with the TM pseudopotential (full lines) are plotted as a function of photon energy (in eV). The vertical lines indicate the energy position of the main peaks dominating the line shape of the cross section measured experimentally (Ref. 39).

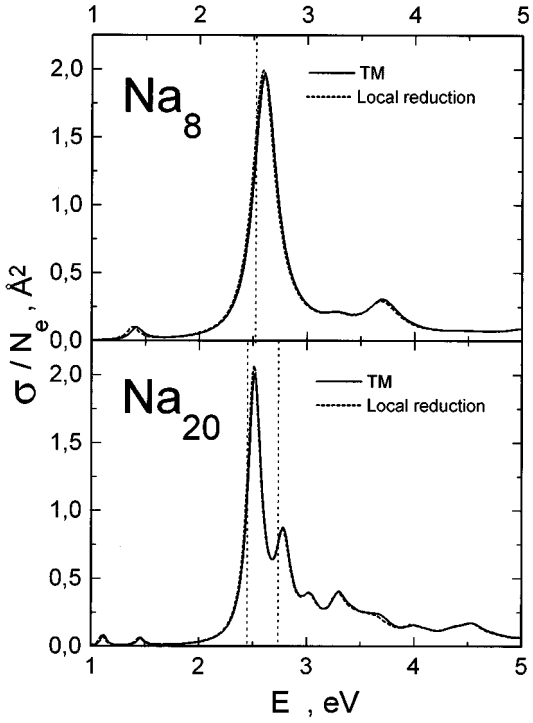

FIG. 5. The photoabsorption cross section per valence electron (in $Å^2$) for the sodium clusters as a function of photon energy (in eV), computed with the TM pseudopotential (full lines) is compared with its local reduction obtained by keeping only the *s*-component of the original TM pseudopotential (dashed lines). Same notation as Fig. 3.

line shape, but also invalidates any plasmon-pole type of argument to interpret the optical properties of small clusters.

We also investigated the role of the nonlocal character of the pseudopotentials in determining the features of the optical response. To this end, we reduce the nonlocal pseudopotentials to a local form, obtained by keeping only the *s*-part of each pseudopotential. We then compute the photoabsorption cross section for the equilibrium geometries already determined in Sec. II. The results are displayed in Fig. 5 for sodium clusters and in Fig. 6 for lithium clusters. In all cases, the static polarizabilities obtained are essentially identical to the ones already displayed in Table I. It becomes clear that, whereas for the sodium clusters the local reduction of the pseudopotential leads to very similar photoabsorption line shapes, for lithium clusters the effect is sizeable for both clusters. Furthermore, as shown in Ref. 2, the nonlocal character of the lithium pseudopotential is responsible for the centered trigonal prism equilibrium geometry for Li_8. In fact, if we neglect the nonlocal term of the lithium pseudopotential, the equilibrium geometry becomes the bicapped octahedron, the same equilibrium geometry of Na_8. Therefore, the local reduction of the pseudopotentials constitutes a good approximation for sodium clusters, but is rather inaccurate for lithium clusters.

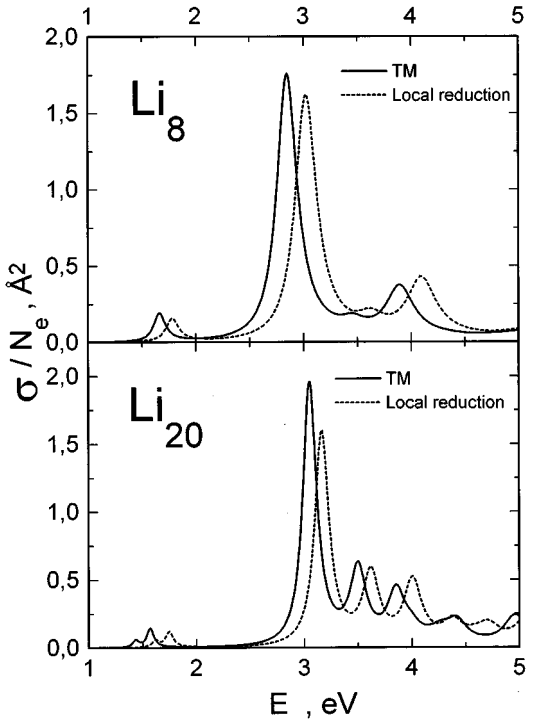

FIG. 6. The photoabsorption cross section per valence electron (in $Å^2$) for the lithium clusters as a function of photon energy (in eV), computed with the TM pseudopotential (full lines) is compared with its local reduction obtained by keeping only the *s*-component of the original TM pseudopotential (dashed lines). Same notation as Fig. 3.

IV. CONCLUSIONS

The equilibrium geometrical shape of alkali metallic clusters obtained via structural minimization in LDA-DFT is found to be independent of the *ab initio* pseudopotentials which are utilized to mimic the role of the constituent atoms. Yet, the effective volume spanned by these equilibrium structures is different, an effect that we traced back to the use of an ionic reference configuration in the construction of the BHS pseudopotential. The static polarizability, which is found to be very sensitive to the effective volume of the cluster, constitutes an excellent candidate to experimentally resolve this issue. Consequently, more experimental measurements of the static polarizability of free metallic clusters are encouraged. The present results suggest that, starting from known geometries, the *s*-part of the nonlocal pseudopotentials are adequate to provide a good estimate of the static polarizability. However, the nonlocal character of the pseudopotentials cannot be ignored in determining the equilibrium geometry of the cluster, as well as in the determination of the line shape of the photoabsorption cross section.

ACKNOWLEDGMENTS

Financial support from FEDER and the PRAXIS XXI program under Contract. No. PRAXIS/2/2.1/FIS/26/94 and from JNICT under Contract No. PBIC/C/FIS/2220/95 are gratefully acknowledged.

[1] W. de Heer, Rev. Mod. Phys. **65**, 611 (1993).
[2] M. W. Sung, R. Kawai, and J. H. Weare, Phys. Rev. Lett. **73**, 3552 (1994).
[3] J. L. Martins, J. Buttet, and R. Car, Phys. Rev. B **31**, 1804 (1985).
[4] U. Röthlisberger and W. Andreoni, J. Chem. Phys. **94**, 8129 (1991).
[5] Y. Wang, D. Tomanck, M. Schlüter, and Caio Lewenkopf, Chem. Phys. Lett. **205**, 521 (1993).
[6] F. Alasia, R. A. Broglia, Ll. Serra, G. Coló, and J. M. Pacheco, J. Phys. B **27**, L643 (1994).
[7] J. M. Pacheco, F. Alasia, H. E. Roman, and R. A. Broglia, Z. Phys. D **37**, 277 (1996).
[8] W. Ekardt, Phys. Rev. Lett. **52**, 1925 (1984); Phys. Rev. B **31**, 6360 (1985); Phys. Rev. B **32**, 1961 (1985).
[9] L. B. Hansen, P. Stoltze, J. K. Norskov, B. S. Clausen, and W. Nieman, Phys. Rev. Lett. **64**, 3155 (1990).
[10] K. K. Verma, J. T. Bahns, A. R. Rajaei-Rizi, W. C. Stwalley, and W. T. Zemke, J. Chem. Phys. **78**, 3599 (1983).
[11] W. B. Pearson, *A Handbook of Lattice Spacings and Structures of Metals and Alloys* (Pergamon, London, 1958).
[12] G. B. Bachelet, D. R. Hamman, and M. Schlüter, Phys. Rev. B **26**, 4199 (1982).
[13] N. Troullier and J. L. Martins, Phys. Rev. B **43**, 1993 (1991).
[14] N. Binggeli, J. L. Martins, and J. R. Chelikowsky, Phys. Rev. Lett. **68**, 1992 (1992).
[15] J. P. Perdew and A. Zunger, Phys. Rev. B **23**, 5048 (1981).
[16] D. M. Ceperley and B. J. Alder, Phys. Rev. Lett. **45**, 566 (1980).
[17] J. M. Pacheco and R. A. Broglia, Phys. Rev. Lett. **62**, 1400 (1989).
[18] Th. Reiners, C. Ellert, M. Schmidt, and H. Haberland, Chem. Phys. Lett. **215**, 357 (1993); Phys. Rev. Lett. **74**, 1558 (1995).
[19] L. Kleinman and D. M. Bylander, Phys. Rev. Lett. **48**, 1425 (1982).
[20] W.-D. Schöne, W. Ekardt, and J. M. Pacheco, Phys. Rev. B **50**, 11 079 (1994).
[21] We have checked that the precise location of the walls does not affect the final results.
[22] C. Yannouleas, E. Vigezzi, and R. A. Broglia, Phys. Rev. B **47**, 9849 (1993).
[23] M. Bernath, M. E. Spina, and J. M. Pacheco, Phys. Rev. B **49**, 10 764 (1994).
[24] We would like to point out the good agreement found between the value obtained in Ref. 33 for Na_8 (1.47), computed in LSDA and including the full anisotropy of the ionic field, and ours (1.44), obtained in TDLDA with a sphericalized ionic contribution.
[25] W. D. Knight, K. Clemenger, W. de Heer, and W. A. Saunders, Phys. Rev. B **31**, 2539 (1985).
[26] The incorporation of thermal effects poses no conceptual problems. Indeed, the method utilized in Ref. 34, if applied making use of $E(\{\mathbf{R}_i\})$ instead of its harmonic approximation around the equilibrium configuration, naturally leads to the temperature dependence of the static (and dynamic) polarizability, as well as the linewidth of the plasmon due to its coupling to the ionic vibrations (Ref. 17).
[27] N. Dam and W. A. Saunders, Z. Phys. D **19**, 85 (1991); Phys. Rev. B **46**, 4205 (1992).
[28] S. G. Louie, S. Froyen, and M. L. Cohen, Phys. Rev. B **26**, 1738 (1982).
[29] I. Moullet, W. Andreoni, and P. Gianozzi, J. Chem. Phys. **90**, 7306 (1989).
[30] J. M. Pacheco, W. Ekardt, and W.-D. Schöne, Europhys. Lett. **34**, 13 (1996).
[31] J. M. Pacheco and W. Ekardt, Ann. Phys. (Leipzig) **1**, 254 (1992).
[32] In all cases, the line shape has been artificially broadened in order to simulate the coupling of the plasmon to the normal vibrations of the cluster. Following the results of Refs. 17 and 35, we used damping ratios $\Gamma=0.1$, 0.06, 0.08, and 0.05 for Na_8, Na_{20}, Li_8, and Li_{20}, respectively, corresponding to carry out the coupling at room temperature.
[33] I. Moullet, J. L. Martins, F. Reuse, and J. Buttet, Phys. Rev. Lett. **65**, 476 (1990); Phys. Rev. B **42**, 11 598 (1990).
[34] M. S. Hansen, J. M. Pacheco, and G. Onida, Z. Phys. D **35**, 149 (1995).
[35] J. M. Pacheco, B. R. Mottelson, and R. A. Broglia, Z. Phys. D **21**, 289 (1991).
[36] I. Moullet, P. Gianozzi, and W. Andreoni (unpublished).
[37] M. M. Dacorogona and M. L. Cohen, Solid State Commun. **55**, 35 (1985).
[38] K. Selby, V. Kresin, J. Masui, M. Vollmer, W. de Heer, A. Scheidemann, and W. Knight, Phys. Rev. B **43**, 4565 (1991).